Inorganic Chemistry

pubs.acs.org/IC Article

Rigid Acridane-Based Pincer Supported Rare-Earth Complexes for *cis*-1,4-Polymerization of 1,3-Conjugated Dienes

Fen You, Jingjing Zhai, Yat-Ming So, and Xiaochao Shi*

Cite This: *Inorg. Chem.* 2021, 60, 1797−1805 Read Online

ACCESS | Metrics & More | Article Recommendations | SI Supporting Information

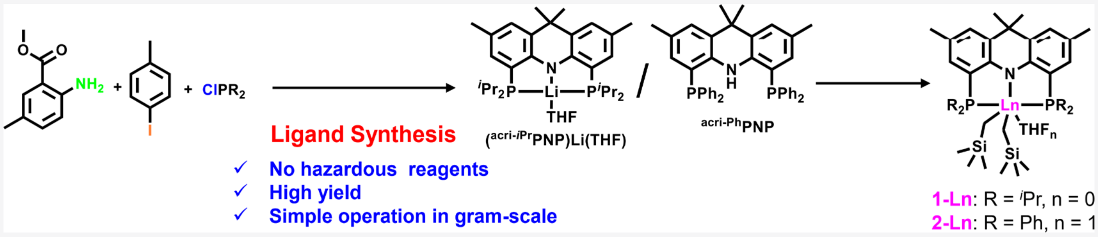

ABSTRACT: A convenient synthetic route has been developed for preparing the novel rigid 4,5-(PR$_2$)2−2,7,9,9-tetramethylacridane-based pincer ligands ($^{acri\text{-}R}$PNP; R = ^{i}Pr and Ph), and the first rare-earth (Ln = Y, Lu) alkyl complexes bearing the $^{acri\text{-}R}$PNP ligands were synthesized by a salt metathesis reaction (for the isopropyl-substituent $^{acri\text{-}iPr}$PNP complexes, **1-Ln**) or direct alkylation (for the phenyl-substituent $^{acri\text{-}Ph}$PNP complexes, **2-Ln**). For both **1-Ln** and **2-Ln**, the NMR spectroscopy and X-ray diffraction study confirmed the successful coordination of the $^{acri\text{-}R}$PNP ligand to the central metal ion in a tridentate manner via the two phosphine and the nitrogen donors. In contrast to **1-Ln** that are solvent-free complexes, the metal centers in **2-Ln** are each coordinated with one tetrahydrofuran molecule. Upon activation by $[Ph_3C][B(C_6F_5)_4]$, **1-Y** and **2-Lu** could catalyze the living polymerization of isoprene and β-myrcene with high catalytic activity and high *cis*-1,4-selectivity (up to 92.3% for isoprene and 98.5% for β-myrcene). Moreover, the **1-Y**/$[Ph_3C][B(C_6F_5)_4]$ catalytic system also could promote the polymerization of butadiene and its copolymerization with isoprene to produce copolymers with high *cis*-1,4-selectivity and narrow polydispersity.

■ INTRODUCTION

Because of its similarity to natural rubber in both chemical composition and stereostructure, the synthetic *cis*-1,4-regulated polyisoprene (PIP) could be a replacement for natural rubber in many fields; polybutadiene (PBD) is another important elastomer or component used for different elastic materials. Copolymers produced by the copolymerization of isoprene (IP) and butadiene (BD) also belong to a type of high-performance synthetic rubber. It is well-known that the synthesis of new polymers with precise microstructure and desired properties crucially relies on the development of new polymerization catalysts. Therefore, in the last half century, the investigations on homogeneous catalytic systems that could provide high *cis*-1,4-selectivity as well as a living mode for the isoprene and butadiene (co)polymerization have spurred extensive research interests and have made considerable progress.[1,2] In particular, rare-earth (denoted as Ln hereafter) complexes have been demonstrated to be efficient catalysts for promoting the *cis*-1,4-polymerization of 1,3-conjugated dienes (isoprene and butadiene, and so on) with high activity and high *cis*-1,4-selectivity.[3] Thus far, a number of rare-earth complexes bearing an aryldiimine ligand (NCN-pincer),[4] half-sandwich cyclopentadienyl,[5] bis(phosphino)amido (PNP-pincer),[6] etc. have been developed for *cis*-1,4-(co)-polymerization of isoprene and butadiene. In spite of their interesting performances in controllable incorporation of other polymeric sequences to modify the resultant polymers, these catalytic systems rarely exhibited a living character with high *cis*-1,4-selectivity. Of note are the bis(phosphino)amido-PNP rare-earth complexes reported by Hou and co-workers (Figure 1a) that could catalyze the living polymerization and copolymerization of isoprene and butadiene with high *cis*-1,4-selectivity (up to 99.6%), without the addition of any

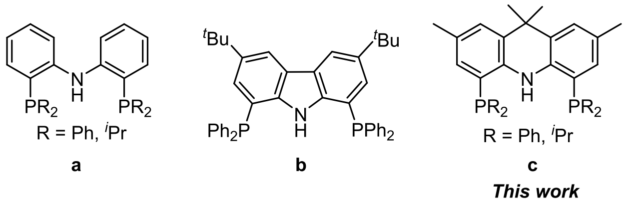

Figure 1. PNP-pincer ligands for rare-earth complexation.

Received: November 4, 2020
Published: January 14, 2021

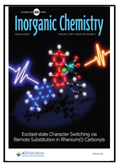

ACS Publications

https://dx.doi.org/10.1021/acs.inorgchem.0c03274
Inorg. Chem. 2021, 60, 1797−1805

aluminum additive.[6a] The yttrium complexes bearing a bis(phosphinophenyl)carbazolyl-PNP pincer ligand (Figure 1b) reported by Cui and co-workers also displayed high *cis*-1,4-selectivity (>99%) for the living polymerization of isoprene.[6b]

Encouraged by the versatile applications of PNP-pincer ligands in the fields of polymerization, small-molecule activation, etc.,[7] as well as specifically the outstanding performances of the bis(phosphino)amido[6a] (Figure 1a) and bis(phosphinophenyl)carbazolyl[6b] (Figure 1b) based PNP-pincer ligands in rare-earth catalyzed polymerization, we embarked on the research of the analogous acridane-based PNP-pincer ligands (Figure 1c; denoted as $^{\text{acri-R}}$PNP hereafter)[8−10] and their complexation to rare-earth metals. Novel acridane-based PNP-pincer ligands ($^{\text{acri-R}}$PNP), that feature a rigid backbone, were reported recently, and remarkably, their corresponding nickel,[8] ruthenium,[9] and titanium[10] complexes exhibited interesting electronic properties and showed unprecedented diverse transformations for small-molecule activation. However, in spite of the fascinating chemistry derived from the $^{\text{acri-R}}$PNP ligand, the complicated synthetic pathways for this ligand render its studies and applications difficult.[8−11] In this work, we have successfully developed a convenient synthetic route to prepare the $^{\text{acri-R}}$PNP ligands (R = ^{i}Pr and Ph) on the gram scale, paving the way for exploration of this novel ligand. Meanwhile, the first rare-earth complexes containing the $^{\text{acri-R}}$PNP ligands have been synthesized, and their high catalytic performances in promoting the *cis*-1,4-selective (co)polymerization of 1,3-conjugated dienes (IP and BD) will be reported. As an immediately available natural conjugated diene and a dimer of isoprene, *β*-myrcene (MY, 7-methyl-3-methylene-octa-1,6-diene, $C_{10}H_{16}$) can be used as a biomonomer for the preparation of biosourced elastomeric materials.[12] In this work, the *cis*-1,4-selective polymerization of *β*-myrcene catalyzed by $^{\text{acri-R}}$PNP-ligated rare-earth complexes will be also investigated.

■ RESULTS AND DISCUSSION

Synthesis of Acridane-Based PNP-Pincer Ligands. The synthesis of the extremely rigid acridane-based $^{\text{acri-R}}$PNP ligands in previous reports was rather complicated, and it involved the use of some difficult-to-handle reagents, such as the carcinogenic diazomethane.[8−11] Taking note that the key step for the synthesis of $^{\text{acri-R}}$PNP ligands involves the preparation of 2,7,9,9-tetramethylacridan,[8,9] in this work, we have developed a more efficient synthetic route to prepare $^{\text{acri-R}}$PNP ligands in five steps (Scheme 1). The Ullmann reaction of commercially available methyl 2-amino-5-methylbenzoate with iodobenzene at 180 °C provided the ligand backbone intermediate, methyl 2-(N-(4-methylphenyl)amino)-5-methylbenzoate, and then the subsequent cyclization reaction via tertiary alcohol formation and an intramolecular Friedel−Crafts alkylation could easily produce the desired key intermediate, namely, 2,7,9,9-tetramethylacridan (H[AH$_2$]), in high yield (total yield 76.8% after three steps). H[AH$_2$] was then brominated in acetic acid to yield the corresponding brominated product (H[ABr$_2$]) quantitatively. H[ABr$_2$] was subsequently operated by deprotonation and salt elimination following the literature method with reasonable modifications to afford the isopropyl-substituted $^{\text{acri-}i\text{Pr}}$PNP ligand and the phenyl-substituted analogue ($^{\text{acri-Ph}}$PNP) in lithium salt and neutral forms, respectively.[8,9] The overall yields of the $^{\text{acri-R}}$PNP-ligands produced by above-described approaches were 40.8% for ($^{\text{acri-}i\text{Pr}}$PNP)Li(THF) (THF = tetrahydrofuran) and 46.3% for $^{\text{acri-Ph}}$PNP. This newly developed synthetic methodology eliminates the tedious synthetic steps as well as the usage of hazardous reagents, thus enabling convenient and scalable synthesis of the novel $^{\text{acri-R}}$PNP ligands for further studies.

Scheme 1. Synthesis of $^{\text{acri-R}}$PNP Pincer Ligands

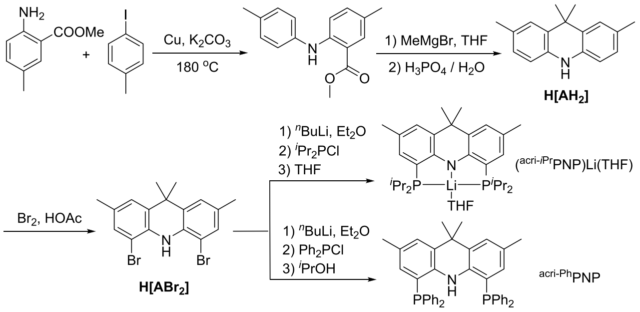

Synthesis of $^{\text{acri-R}}$PNP Ligated Rare-Earth Dialkyl Complexes. With the $^{\text{acri-R}}$PNP ligands in hand, we attempted to synthesize the corresponding rare-earth dialkyl complexes by using the suitable ligands (Scheme 2). The isopropyl-substituted $^{\text{acri-}i\text{Pr}}$PNP complexes [($^{\text{acri-}i\text{Pr}}$PNP)Ln(CH$_2$SiMe$_3$)$_2$] (Ln = Y (**1-Y**), 68.7% yield; Ln = Lu (**1-Lu**), 63.4% yield) were prepared via metathesis reaction of ($^{\text{acri-}i\text{Pr}}$PNP)Li(THF) with LnCl$_3(THF)_x$ (Ln = Y, x = 3.5; Ln = Lu, x = 3) followed by alkylation with 2 equiv of Me$_3$SiCH$_2$Li. The NMR (^{1}H and ^{31}P) spectra revealed the negligible decomposition of **1-Y** at room temperature for 24 h (Figure S20). For the phenyl-substituted $^{\text{acri-Ph}}$PNP, direct deprotonation of the ligand by yttrium and lutetium trialkyl precursors Ln(CH$_2$SiCH$_3$)$_3$(THF)$_3$ afforded the targeted dialkyl complexes [($^{\text{acri-Ph}}$PNP)Ln(CH$_2$SiMe$_3$)$_2$(THF)] (Ln = Y (**2-Y**), 50.7% yield; Ln = Lu (**2-Lu**), 50.2% yield). The ^{1}H NMR spectra of **2-Ln** clearly indicated the presence of a coordinated THF molecule, while those of **1-Ln** displayed the solvent-free coordination environment. It is noteworthy that the synthesis of yttrium complex **2-Y** could be accomplished smoothly at room temperature in 2 h, whereas for **2-Lu**, a higher reaction temperature of 50 °C was required for

Scheme 2. Synthesis of the $^{\text{acri-R}}$PNP Ligated Rare-Earth Complexes

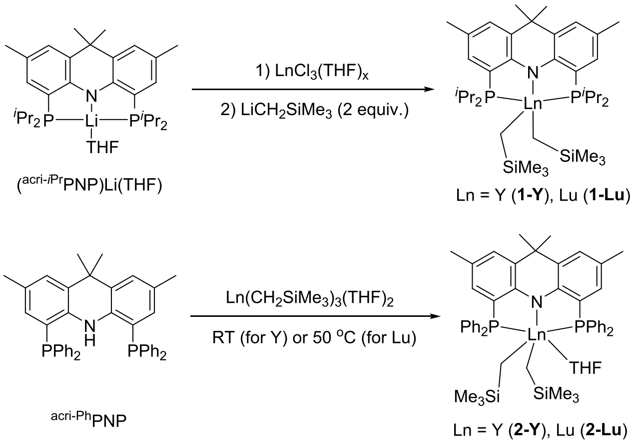

complete reaction. ^{31}P NMR analysis was used to monitor the progress of the synthesis of **2-Lu** (Figure 2). When the reaction was performed at room temperature for 5 h, the ^{31}P NMR signals assigned to **2-Lu** (δ − 7.5 ppm) and precursor $^{\text{acri-Ph}}$PNP pro-ligand (δ − 23.6 ppm) coexisted (Figure 2b), indicating that the reaction was incomplete. On the other hand, complete reaction was achieved when the reaction was conducted at 50 °C after 2 h (Figure 2c). Moreover, a doublet with distinct Y−P coupling was observed in the ^{31}P NMR spectrum of the yttrium complex ($J_{\text{Y−P}}$ = 85.9 Hz for **1-Y** and $J_{\text{Y−P}}$ = 47.0 Hz for **2-Y**), indicating that the acridane-based ligand coordinates to the cationic yttrium center via the phosphine atoms.[6]

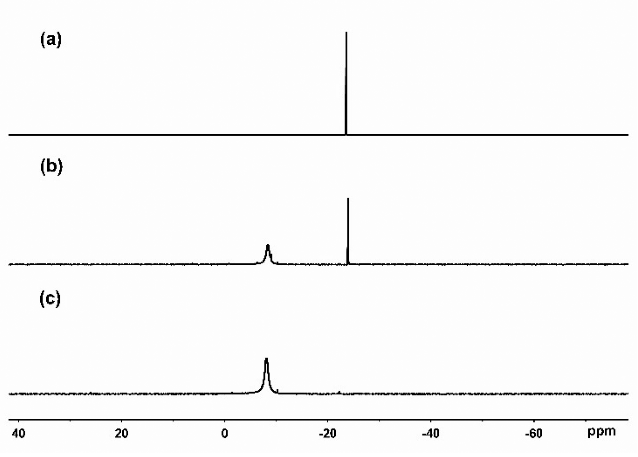

Figure 2. ^{31}P NMR spectrum in monitoring the formation of **2-Lu** at different reaction temperature (162 MHz, C_6D_6, 25 °C). (a) $^{\text{acri-Ph}}$PNP; (b) reaction of $^{\text{acri-Ph}}$PNP with $Lu(CH_2SiMe_3)_3(THF)_2$ for 5 h at room temperature; (c) reaction of $^{\text{acri-Ph}}$PNP with $Lu(CH_2SiMe_3)_3(THF)_2$ for 2 h at 50 °C.

The solid-state structures of complexes **1-Y** and **2-Lu** were established by X-ray diffraction and are depicted in Figures 3 and 4, respectively. The Y(III) center in **1-Y** is five-coordinated with the tridentate $^{\text{acri-}i\text{Pr}}$PNP ligand and two trimethylsilylmethyl groups, whereas the Lu(III) center in **2-Lu** is six-coordinated with the $^{\text{acri-Ph}}$PNP ligand, two trimethylsilylmethyls, and a THF molecule. For both **1-Y** and **2-Lu**, the respective tridentate acridane-based pincer ligand binds to the central metal ion via the two phosphine and the nitrogen atoms. In contrast to their transition-metal congeners, e.g., Ni-,[8] Ru-,[9] and Ti-$^{\text{acri-R}}$PNP[10] complexes, that exhibited coplanar binding mode of the $^{\text{acri-R}}$PNP ligand to the metal center, the Ln(III) metal centers in both **1-Y** and **2-Lu** are extruded out-of-plane from the corresponding $^{\text{acri-R}}$PNP ligands, which could be attributed to the relatively larger metal ionic size of Ln(III) centers that render them unable to be coordinated coplanarly inside the acridane-based PNP cavity. On the other hand, the analogous rare-earth complexes supported by the bis(phosphinophenyl)carbazolyl-PNP pincer ligand (Figure 1b) exhibit a pseudo-coplanar coordination mode,[6b] highlighting the more steric congestion in $^{\text{acri-R}}$PNP when compared with the bis(phosphinophenyl)carbazolyl-PNP pincer. The present configurations of **1-Y** and **2-Lu** resemble that of the flexible bis(phosphinophenyl)amido-ligated rare-earth analogues,[6a] but with a much more rigid PNP backbone. The bond lengths of Y−N1(amido) in **1-Y** and Lu−N1(amido) in **2-Lu** are 2.3691(16) and 2.345(4) Å, respectively, while the average Y−P(phosphine) bond and the average Lu−P(phosphine) bond distances are 2.8912 and 2.9432 Å, respectively. The metal-amido and metal-phosphine bonds in both **1-Y** and **2-Lu** are comparable with those reported in the analogous rare-earth complexes supported by carbazolide-PNP[6a] and bis(phosphinophenyl)amido[6b] ligands.

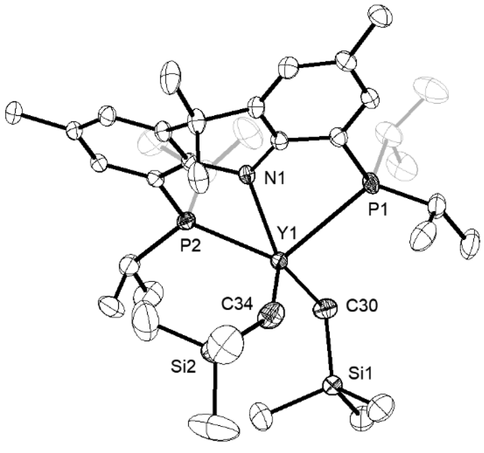

Figure 3. X-ray molecular structure of **1-Y** with 40% probability thermal ellipsoids. Hydrogen atoms and the solvent molecule are omitted for clarity. Selected bond distances (Å) and angles (deg): Y1−N1 2.3691(16), Y1−P1 2.8897(5), Y1−P2 2.8926(5), Y1−C30 2.422(2), Y1−C34 2.349(2); N1−Y1−C30 146.41(6), C34−Y1−C30 113.59(9), N1−Y1−P1 69.52(4), N1−Y1−P2 69.75(4), P1−Y1−P2 115.360(15).

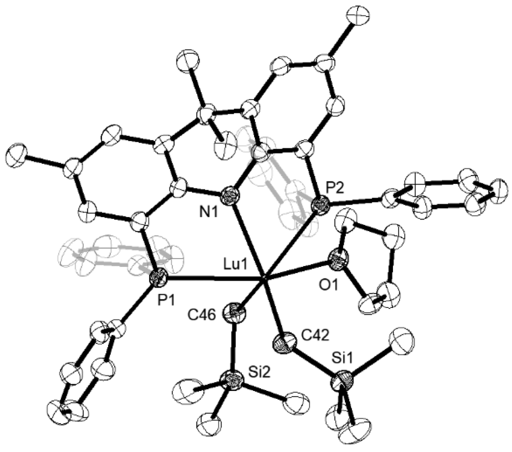

Figure 4. X-ray molecular structure of **2-Lu** with 40% probability thermal ellipsoids. Hydrogen atoms and the solvent molecule are omitted for clarity. Selected bond distances (Å) and angles (deg): Lu1−N1 2.345(4), Lu1−C42 2.357(6), Lu1−C46 2.380(5), Lu1−P1 2.9037(14), Lu1−P2 2.9827(13), Lu1−O1 2.323(4); O1−Lu1−N1 96.22(15), N1−Lu1−C42 139.34(19), O1−Lu1−C46 84.80(18), N1−Lu1−C46 101.33(18), C42−Lu1−C46 112.7(2), O1−Lu1−P1 161.33(10), N1−Lu1−P1 68.47(11), N1−Lu1−P2 67.28(11), P1−Lu1−P2 105.97(4).

Polymerization of Isoprene. In view of the good efficiency of the reported PNP-pincer rare-earth analogues for 1,3-conjugeted diene polymerization,[6] the catalytic performances of **1-Ln** and **2-Ln** toward polymerization of isoprene have been explored, and the representative results are summarized in Table 1. In the presence of activator $[Ph_3C][B(C_6F_5)_4]$ (B), **1-Y** that bears the isopropyl-substituted $^{\text{acri-}i\text{Pr}}$PNP could polymerize 500 equiv of isoprene

Table 1. Polymerization of Isoprene and β-Myrcene by 1-Ln and 2-Ln under Various Conditions[a]

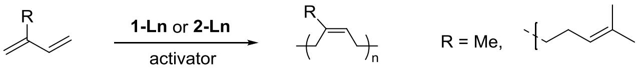

entry	cat.	[act.]	Mon.[b]	[M]/[Ln]	T (°C)	t (min)	yield (%)	microstructure[c]			M_n[d] (× 104 g/mol)	M_w/M_n[d]	eff.[e] (%)
								cis-1,4	*trans*-1,4	3,4-			
1	**1-Y**	**A**	IP	500	25	10	54.7	90.2		9.8	7.87	1.10	23.7
2	**1-Y**	**B**	IP	500	25	5	>99	89.3		10.7	6.22	1.04	54.7
3	**1-Y**	**C**	IP	500	25	240							
4	**1-Lu**	**A**	IP	500	25	10	56.8	63.8		36.2	6.33	1.03	30.5
5	**1-Lu**	**B**	IP	500	25	5	87.8	66.4		33.6	5.51	1.06	54.3
6	**1-Lu**	**B**	IP	500	25	10	>99	61.2		38.8	6.14	1.02	55.5
7	**1-Lu**	**C**	IP	500	25	240							
8	**2-Lu**	**A**	IP	500	25	10	82.6	82.0	2.4	15.6	8.40	1.04	33.5
9	**2-Lu**	**B**	IP	500	25	600	27.5	79.2	4.0	16.8	3.04	1.01	30.8
10	**2-Lu**	**C**	IP	500	25	600							
11	**2-Y**	**A**	IP	500	25	50	94.5	50.5		49.5	10.4	1.05	30.9
12	**2-Y**	**B**	IP	500	25	750	33.7	47.2	10.2	42.6	4.14	1.02	27.7
13	**1-Y**	**B**	IP	350	25	8	>99	89.0		11.0	3.86	1.04	61.8
14	**1-Y**	**B**	IP	750	25	30	>99	86.7		13.3	8.41	1.03	60.7
15	**1-Y**	**B**	IP	1000	25	60	>99	88.3		11.7	11.1	1.03	61.4
16	**1-Y**	**B**	IP	1500	25	120	>99	88.6		11.4	16.8	1.03	60.8
17	**1-Y**	**B**	IP	1000	25	0.5	21.6	84.3		15.7	2.62	1.03	56.2
18	**1-Y**	**B**	IP	1000	25	1.6	41.8	87.8		12.2	4.91	1.03	58.0
19	**1-Y**	**B**	IP	1000	25	2	49.4	83.3		16.7	5.51	1.06	61.1
20	**1-Y**	**B**	IP	1000	25	3	62.9	83.6		16.4	6.95	1.02	61.6
21	**1-Y**	**B**	IP	1000	25	4	80.3	86.7		13.3	9.02	1.03	60.6
22	**1-Y**	**B**	IP	500	0	60	70.8	92.3		7.7	7.71	1.04	31.3
23	**1-Y**	**B**	IP	500	50	3	>99	84.1	1.9	14	6.23	1.03	54.7
24	**1-Y**	**B**	IP	500	80	1	83.4	79.5	4.1	16.4	6.30	1.02	45.1
25	**1-Y**	**B**	IP	500	80	3	>99	79.3	4	16.7	7.13	1.03	47.8
26	**1-Y**	**B**	IP	500 + 500	25	10 + 10	>99	89.2		10.8	10.09	1.03	67.5
27	**1-Y**	**B**	MY	500	25	6	73.4	98.0		2.0	6.63	1.06	75.4
28	**1-Y**	**B**	MY	500	25	10	>99	97.8		2.2	8.92	1.06	76.3
29	**1-Y**	**B**	MY	1000	25	20	>99	98.5		1.5	18.2	1.04	72.5
30	**1-Y**	**B**	MY	500	80	5	74.1	96.9		3.1	8.51	1.07	59.3
31	**1-Lu**	**B**	MY	500	25	10	27.3	78.5		21.5	3.48	1.04	53.4
32	**2-Y**	**A**	MY	500	25	60	34.5	63.1		36.9	6.95	1.02	33.8
33	**2-Lu**	**A**	MY	500	25	10	65.5	92.4		7.6	9.37	1.07	47.6

[a] Conditions: toluene (6 mL); catalyst (20 umol); [Ln]/[act.] = 1:1 ([act.] = $[PhMe_2NH][B(C_6F_5)_4]$ (**A**), $[Ph_3C][B(C_6F_5)_4]$ (**B**), $B(C_6F_5)_3$ (**C**)). [b] Mon: IP = isoprene, MY = β-myrcene. [c] Measured by means of ^1H NMR and ^{13}C NMR spectroscopy in $CDCl_3$. [d] Determined by gel permeation chromatography (GPC) against polystyrene standards at 35 °C. [e] Catalyst efficiency = M_n (calculated)/M_n (measured).

quantitatively in 5 min to afford the polyisoprene with high *cis*-1,4-seletivity (88.3% *cis*-1,4) and narrow molecular weight distribution (M_w/M_n = 1.02; Table 1, Entry 2). Another borate salt $[PhMe_2NH][B(C_6F_5)_4]$ (A) could also serve as an efficient activator for **1-Y** (Table 1, entry 1), while the neutral borane compound $B(C_6F_5)_3$ was inactive (Table 1, entry 3). Notably, **1-Y** catalyzed the polymerization of isoprene in a living manner (Figure 5). At a monomer feed of 1000, as the reaction time prolonged, the conversion increased, and the molecular weight of resultant polymers increased linearly from 2.62×10^4 to 11.1×10^4 g/mol with narrow molecular weight distribution ($M_w/M_n < 1.10$, Figure 5a and Table 1, runs 2, 13–17). The molecular weights of the resulting polymers also increased linearly with the monomer feeding ratios varying from 350 to 1500 (Figure 5b and Table 1, entries 2, 9–12). Additionally, when another portion of isoprene (500 equiv) was added to a terminative catalytic polymerization system, the molecular weight of the resulting polymer was doubled with the molecular-weight distribution remaining narrow (M_w/M_n = 1.03, Table 1, entry 20), which implied the long lifetime of active polymeric chain ends. All of the above observations indicated that the **1-Y** catalyzed polymerization of isoprene proceeded in a living manner (Figure 5). In addition, when the isoprene polymerization by the **1-Y**/$[Ph_3C][B(C_6F_5)_4]$ system was carried out at a low temperature (i.e., 0 °C), improved regio- and stereoselectivity of the resulting polymer (92.3% *cis*-1,4) were observed (Table 1, entry 18). Remarkably, the high catalytic activity of **1-Y**/$[Ph_3C][B(C_6F_5)_4]$ was maintained well when the reaction temperature was even increased to 80 °C, so that it could polymerize 500 equiv of isoprene quantitatively in 3 min but with slightly decreased *cis*-1,4-selectivity (Table 1, entries 23–25). These results clearly suggested the thermal stability of the active species in this $^{acri\text{-}R}$PNP rare-earth catalytic systems.[6] In all of the isoprene polymerization cases, the **1-Y**/$[Ph_3C][B(C_6F_5)_4]$ catalytic system showed moderate initiation efficiencies (31.3–67.5%). Compared with **1-Y**, the lutetium analogue **1-Lu** also exhibited high catalytic activity, but with a rather lower stereoselectivity

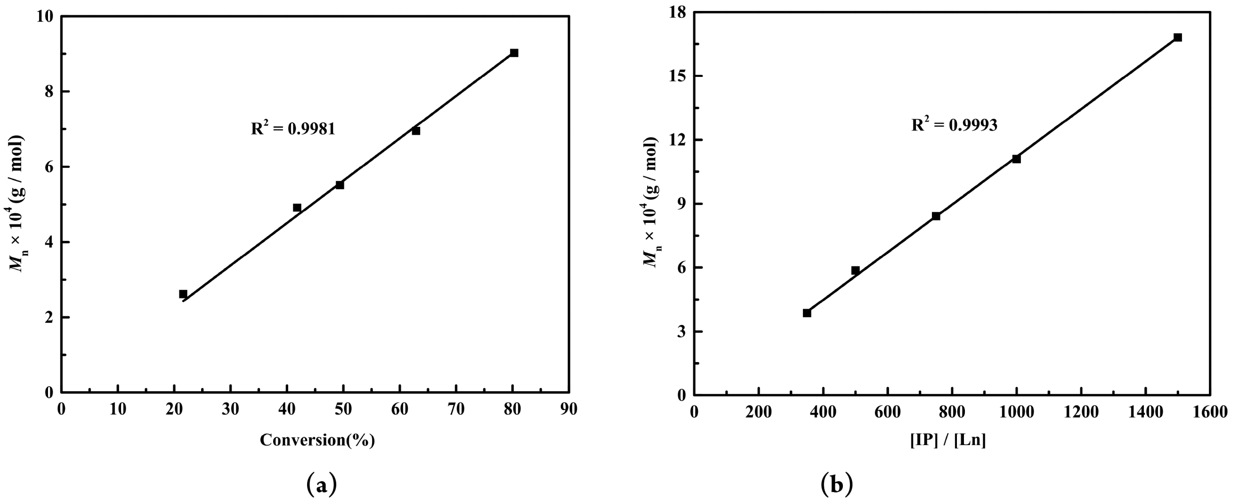

Figure 5. (a) Polymerization of isoprene with **1-Y**/[$(Ph_3C)(B(C_6F_5)_4)$] as a precursor: molecular weight vs conversion. (b) Polymerization of isoprene with **1-Y**/[$(Ph_3C)(B(C_6F_5)_4)$] as a precursor: molecular weight vs isoprene-to-[**1-Y**] ratio.

Table 2. Copolymerization of Butadiene and Isoprene using 1-Y/[Ph_3C][$B(C_6F_5)_4$][a]

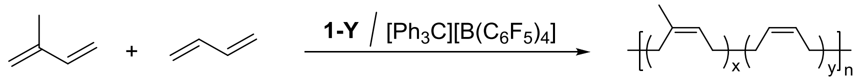

			microstructure[c]			
entry	[BD]/[IP]/[Ln]	BD in polymer[b] (mol %)	*cis*-1,4/*trans*-1,4/1,2-BD	*cis*-1,4/*trans*-1,4/3,4-IP	M_n[d] (× 10^3 g/mol)	M_w/M_n[d]
1	2000/0/1	100	90.2/6.3/3.4		49.9	1.30
2	1600/400/1	85.1	91.7/-/8.3	92.8/-/7.2	61.2	1.25
3	1200/800/1	62.3	94.5/-/5.5	92.6/-/7.4	60.0	1.25
4	1000/1000/1	55.2	92.2/-/7.8	92.6/-/7.4	50.8	1.25
5	800/1200/1	41.4	91.4/-/8.6	92.7/-/7.3	52.7	1.20
6	400/1600/1	23.2	91.1/-/8.9	93.3/-/6.7	66.7	1.12
7	0/2000/1	0		89.8/-/10.2	42.3	1.02

[a] Conditions: toluene (10 mL), room temperature, catalyst (5 umol); [Ln]/[Ph_3C][$B(C_6F_5)_4$] = 1:1, all polymers achieved the conversion rate of around 100. [b] BD in polymer % = $1/2(I_{5.35} + I_{4.95})$ $(1 + I_{5.12} + 1/2I_{4.70})$ in ^{1}H NMR spectra. [c] Measured by means of ^{1}H NMR and ^{13}C NMR spectroscopy in $CDCl_3$. [d] Determined by gel permeation chromatography (GPC) against polystyrene standards at 35 °C.

(*cis*-1,4 = 61.2%) under the optimal polymerization conditions (Table 1, entry 4). The larger ionic radius of the metal center and the resulting more open coordination sphere for isoprene in **1-Y** may be the main reason for its higher stereoselectivity than **1-Lu**. Interestingly, the catalytic performances of **2-Ln** (bearing phenyl-substituted $^{\text{acri-Ph}}$PNP) were substantially different from those of **1-Ln**: higher *cis*-1,4-stereoselectivity was observed for **2-Lu** catalyzed polymerization (82.0% *cis*-1,4) when compared with that of **2-Y** (50.5% *cis*-1,4; Table 1, entries 5 and 8). These results suggested that the R-group substituent on $^{\text{acri-R}}$PNP, together with the Ln center, determine the stereoselectivity of isoprene polymerization. Despite the detailed reasons being currently unclear for the different metal-dependent selectivities in **1-Ln** and **2-Ln** catalytic systems, it is believed that the coordinated-THF molecule plays an important role in the regio- and stereo-selective polymerization of isoprene catalyzed by **2-Ln** (the attempt to obtain the **2-Ln** analogue without coordinated-THF was failed). Yet, additional work (e.g., computational study) is underway to elucidate the stereoselectivity of isoprene polymerization catalyzed by **1-Ln** and **2-Ln**. Furthermore, compared to their analogues bearing bis(phosphino)amido[6a] and bis(phosphinophenyl)carbazolyl ligands,[6b] **1-Ln** and **2-Ln** exhibited comparable catalytic activity for the isoprene polymerization though with slightly lower *cis*-1,4-selectivity, which could be attributed to the rigid and sterically more congested acridane-based ligand.

To elucidate the probable catalytic pathway in the isoprene polymerization, we first performed the reaction of yttrium complex **1-Y** with one equivalent of [Ph_3C][$B(C_6F_5)_4$] in C_6D_6 at 25 °C by NMR spectroscopic techniques. As indicated by the ^{1}H NMR spectrum, the appearance of new signals assignable to [($^{\text{acri-}i\text{Pr}}$PNP)Y($CH_2SiMe_3$)]$^+$ was observed when the borate [Ph_3C][$B(C_6F_5)_4$] abstracted the alkyl moiety $-CH_2SiMe_3$ in **1-Y** (Figure S13). The signals of **1-Y** in the ^{31}P NMR spectrum at δ 1.66 ppm (J_{Y-P} = 86.5 Hz) shifted downfield to δ 2.90 ppm (J_{Y-P} = 95.8 Hz) after the addition of the borate (Figure S14). Moreover, the ^{1}H NMR spectrum of PIP the oligomer clearly suggested the existence of the initiating $-CH_2SiMe_3$ group, by the signals at δ 0 ppm for $-Si\mathit{Me}_3$ and δ 0.57 ppm for the methylene group $-\mathit{CH}_2SiMe_3$ (Figure S15). According to previous reports,[6] the probable catalytic pathway for the polymerization could be simplified as shown in Scheme S1: the alkyl abstraction of **1-Y** with [Ph_3C][$B(C_6F_5)_4$] generates the cationic active species [($^{\text{acri-}i\text{Pr}}$PNP)Y($CH_2SiMe_3$)]$^+$. The *cis*-$\eta^4$ coordination of the isoprene monomer to the cationic active species and the following insertion into the Y-CH_2 bond forms the cationic yttrium isoproprenyl species, which could further propagate to the cationic yttrium-polyisoprene species.

On the basis of the study of isoprene, it is of interest to investigate the catalytic performance of the **1-Ln** and **2-Ln** on the polymerization of β-myrcene (MY), which is a 1,3-diene analogue to isoprene. At room temperature, the **1-Y**/[Ph_3C][$B(C_6F_5)_4$] could convert 500 equiv of MY with a yield of 73.4% in 6 min to produce high *cis*-1,4-selective polymyrcene (PMY, 98.0% *cis*-1,4).[12] Compared to the isoprene polymerization, the relatively lower catalytic activity is probably caused by the long side-substituent in MY that hinders the coordination of the monomer to some extent. However, the long side substituent in MY is also considered as a main reason for its higher *cis*-1,4 selectivity; the interaction of MY with the rigid and bulky ligand in **1-Y** might render the coordination of the monomer from a special direction which is a benefit for enhancing the *cis*-1,4 selectivity. The narrow molecular weight distribution (M_w/M_n < 1.10) suggested that the polymerization preceded in a living manner. Also, the high thermostability of the active species allowed the polymerization of MY at high temperatures, and a yield of 74.1% was obtained in 5 min at 80 °C (Table 1, entry 30). **2-Lu**/[$PhMe_2NH$][$B(C_6F_5)_4$] also catalyzed the polymerization of MY efficiently with high *cis*-1,4 selectivity (92.4%, Table 1, entry 33). Moreover, akin to the cases in isoprene polymerization, similar metal-dependent selectivities were also observed in **1-Ln** and **2-Ln** catalyzed MY polymerizations, of which the resultant PMY catalyzed by **1-Lu** and **2-Y** possessed relatively lower *cis*-1,4 selectivity (Table 1, entries 31 and 32).

(Co)polymerization of Isoprene and Butadiene. The complex **1-Y** also served as an efficient catalyst for the polymerization of butadiene as well as the copolymerization of BD and IP to produce high *cis*-1,4-selective (co)polymers (Table 2).[6b] For the copolymerization of BD and IP, the sequence content of polybutadiene and polyisoprene could be easily adjusted by the addition of different feed ratios of IP/BD; for example, when the monomer feeds of butadiene decreased, the corresponding sequence content of PBD in the resultant copolymers also decreased accordingly. Both butenyl and isopentenyl sequences in the copolymers showed high *cis*-selectivity (>90%), and the M_w/M_n remained narrow (M_w/M_n < 1.30). The Fineman−Ross plot for the copolymerization of IP and BD performed at room temperature was plotted as shown in Figure 6. The plot of $F(f-1)/f$ showed a straight line with the F^2/f as the abscissa, and the monomer competitive polymerization rates were calculated to be r_{BD} = 7.04 and r_{IP} = 0.46, indicating a much higher activity of BD than that of IP. In our trials, the monomer feed ratios ranged from 0.25 to 4, showing that the resultant copolymers mainly possessed gradient/tapered distributions.

CONCLUSION

In conclusion, we have developed a convenient and efficient synthetic route to prepare the novel acridane-based $^{acri\text{-}R}$PNP pincer ligands by facilitating access to the key intermediate H[AH_2] and avoiding the use of difficult-to-handle reagents. This paves a smooth synthetic pathway for the exploration of metal complexes bearing the interesting acridane-based PNP pincer ligand. The first $^{acri\text{-}R}$PNP-ligated rare-earth complexes have been synthesized and structurally characterized. With a suitable organoborate activator, the isopropyl substituted **1-Y** and phenyl substituted **2-Lu** could catalyze the polymerization of isoprene and β-myrcene with high catalytic activity and high *cis*-1,4-selectivity in a living manner. The **1-Y**/[Ph_3C][$B(C_6F_5)_4$] system also could promote the copolymerization of isoprene and butadiene to afford copolymers with high *cis*-1,4-selectivity and well-defined sequence distribution. Given the peculiar reactivity of $^{acri\text{-}R}$PNP-ligated transition metal complexes toward small molecule activation,[8−10] one would expect the fascinating chemistry derived from the rare-earth congeners. Work is currently in progress in that direction.

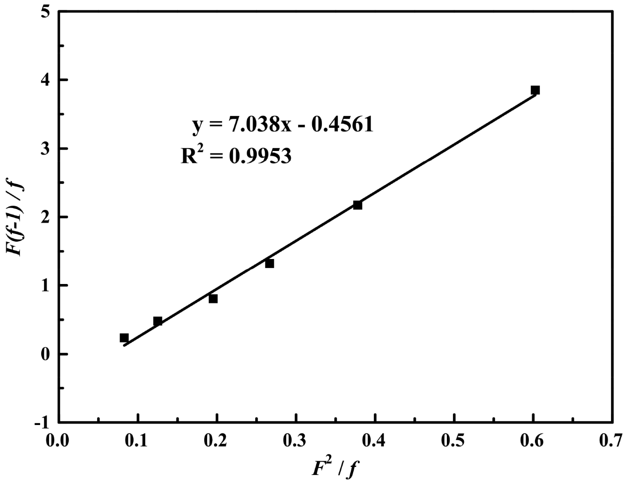

Figure 6. Fineman−Ross plot for copolymerization of butadiene (BD) and isoprene (IP) with **1-Y**/[Ph_3C][$B(C_6F_5)_4$] at 25 °C (F = [BD]/[IP] in feed, f = [BD]/[IP] in copolymer, r_{BD} = 7.03, r_{IP} = 0.46).

EXPERIMENTAL SECTION

General Methods. All air- and moisture-sensitive manipulations were carried out using standard Schlenk line or glovebox (Vigor) techniques under a N_2 atmosphere. Toluene, diethyl ether, and hexane were preprocessed by Solvent Purification System (Vigor), and THF was distilled from sodium-benzophenone. Reagents were purchased from TCI or Aladdin and used without further purification unless there were additional instructions. Isoprene was purchased from Aladdin and purified by distillation over CaH_2, degassed, and stored in a glovebox at −30 °C. The molecular weight and molecular weight distribution of the polymers were measured by Waters 1515 GPC at 35 °C using THF as an eluent (the flow rate is 1 mL/min) against polystyrene standards. ^1H, ^{13}C, and ^{31}P NMR spectra were obtained on a JNM-ECZ400S/L 400 NMR spectrometer and referenced to residual solvent resonances (25 °C). The X-ray intensity data for the complexes were collected with a Bruker D8 Venture system with the ω-scan technique. The structures were solved using direct methods, and further refinements with full-matrix least-squares on F^2 were performed using the SHELXTL program package. Crystallographic data (excluding structure factors) for the structure analysis have been deposited with the Cambridge Crystallographic Data Centre, CCDC 2042088 (**1-Y**) and 2042089 (**2-Lu**). A summary of the crystallographic data for **1-Y** and **2-Lu** is presented in Table S1.

Methyl 5-Methyl-2-(p-tolylamino)benzoate. A mixture of methyl 2-amino-5-methylbenzoate (12.4 g, 75 mmol), iodobenzene (16.4 g, 75 mmol), copper powder (720 mg, 11.3 mmol), and K_2CO_3 (10.4 g, 75 mmol) was heated to 180 °C with stirring for 10 h. When the reaction mixture was cooled down to room temperature, 150 mL of chloroform was added, filtered with Celite, and evaporated to dryness. Pure product was isolated as a yellow solid by column chromatography on silica gel using EtOAc/*n*-hexane = 40:1 as an eluent (19.1 g, 99.5%). Analytical and spectroscopic data for this compound have been published previously.[11]

H[AH$_2$]. MeMgBr (3 M in Et$_2$O, 72 mL, 216 mmol) was added dropwise to a solution of methyl 5-methyl-2-(p-tolylamino)benzoate (16.2 g, 63.3 mmol) in THF (150 mL) at 0 °C, and the reactant mixture was warmed slowly to RT and stirred overnight. The reaction was quenched by the addition of a large amount of water, extracted with Et$_2$O, and dried over anhydrous Na$_2$SO$_4$. After removing the solvent, a yellow oil was obtained which was used in the next step without further purification.

A mixture of 85% H$_3$PO$_4$ (100 mL) and the above yellow oil was heated to 120 °C with stirring for 2 h. After being quenched with water, the mixture was neutralized using a 1 M NaOH solution and extracted with Et$_2$O. The combined organic layers were dried over anhydrous Na$_2$SO$_4$. After filtration and evaporation, the crude product was purified by column chromatography on silica gel (EtOAc/*n*-hexane = 50:1) to give H[AH$_2$] (3,6,9,9-tetramethyl-9,10-dihydroacridine) as a yellow solid (12.5 g, 81.0%). Analytical and spectroscopic data for this compound have been published previously.[11]

H[ABr$_2$]. Br$_2$ was added dropwise to a solution of H[AH$_2$] (9 g, 37.9 mmol) in acetic acid (100 mL) at 0 °C. After slowly being warmed to RT, the mixture was further stirred for 2 h. The reaction was quenched by the addition of a solution of Na$_2$S$_2$O$_3$, and the target product H[ABr$_2$] was obtained through filtration as a green solid (yield = 14.2 g, 95.3%). ^{1}H NMR (400 MHz, CDCl$_3$): δ 7.38 (s, Ph-N*H*-, 1H), 7.20−7.09 (s, Ph-*H*, 4H), 2.28 (s, Ph−C*H*$_3$, 6H), 1.53 (s, C(C*H*$_3$)$_2$, 6H).

($^{acri\text{-}iPr}$PNP)Li(THF). ^{n}BuLi (2.5 M, 6 mL, 15 mmol) was slowly added to a solution of H[ABr$_2$] (1.96 g, 5 mmol) in Et$_2$O at −78 °C. The solution was slowly warm to RT and further stirred for 3 h. The solution was cooled down again to −78 °C, and ^{i}Pr$_2$PCl (1.52 g, 10 mmol) was added into the reaction dropwise. The mixture was stirred for 30 min at −78 °C and then warmed to RT for another 36 h. The solution was concentrated under reduced pressure, and the residue was dissolved in toluene. After the white precipitate filtered off, a clear toluene solution was obtained, and another portion of THF (5 mL) was added and stirred for 30 min. The solvent was removed under reduced pressure, and the crude product was purified by washing with *n*-hexane to afford ($^{acri\text{-}iPr}$PNP)Li(THF) as a light yellow solid (yield = 1.3 g, 55.7%). ^{1}H NMR (C$_6$D$_6$, 400 MHz, ppm) δ 7.30−6.97 (m, Ph-*H*, 4H), 3.47 (t, *THF*, 4H), 2.42 (s, 6H, Ph−C*H*$_3$), 2.15−1.98 (m, 4H, C*H*(CH$_3$)$_2$), 1.71 (s, 6H, Ph$_2$C(C*H*$_3$)$_2$), 1.17 (dd, 16H, *THF* and CH(C*H*$_3$)$_2$), 1.06 (dd, 12H, CH(C*H*$_3$)$_2$). ^{31}P NMR (C$_6$D$_6$, 162 MHz, ppm): δ − 3.7 (d, *J* = 55.1 Hz), − 3.0 (d, *J* = 55.1 Hz).

$^{acri\text{-}Ph}$PNP. ^{n}BuLi (2.5 M, 6 mL, 15 mmol) was slowly added to a solution of H[ABr$_2$] (1.96 g, 5 mmol) in Et$_2$O at −78 °C. After being slowly warmed to RT and further stirring for 3 h, the solution was cooled down again to −78 °C, and Ph$_2$PCl (2.2 g, 10 mmol) was added into the reaction mixture dropwise. The mixture was stirred for 30 min at −78 °C and then warmed to room temperature for another 36 h. The reaction was quenched by the addition of ^{i}PrOH, and the solvent was removed under reduced pressure to afford light-yellow oil. The pure product $^{acri\text{-}Ph}$PNP was isolated as an off-white solid by crystallization from the *n*-hexane solution (1.9 g, 63.3%). ^{1}H NMR (400 MHz, C$_6$D$_6$, ppm): δ 8.71 (s, 1H, Ph-N*H*-), 7.43−6.94 (s, 24H, Ph-*H*), 2.05 (s, 6H, Ph−C*H*$_3$), 1.54 (s, 6H, C(C*H*$_3$)$_2$). ^{31}P NMR (C$_6$D$_6$, 162 MHz, ppm): δ − 23.6.

*($^{acri\text{-}iPr}$PNP)Y(CH$_2$SiMe$_3$)$_2$ (**1-Y**).* In the glovebox, a mixture of ($^{acri\text{-}iPr}$PNP)Li(THF) (285.3 mg, 0.6 mmol) and YCl$_3$(THF)$_{3.5}$ (268.6 mg, 0.6 mmol) in toluene was stirred at room temperature for 1.5 h, and then the toluene solution of LiCH$_2$TMS (113.0 mg, 1.2 mmol) was added to the reaction mixture. Solvent was removed in a vacuum after 2 h, and the desired product ($^{acri\text{-}iPr}$PNP)Y(CH$_2$SiMe$_3$)$_2$ (**1-Y**) was obtained as light-yellow powder (301.7 mg, 68.7%). Upon cooling to −30, light-yellow single crystals of complex **1-Y** were isolated from its saturated toluene/*n*-hexane solution after several days. ^{1}H NMR (C$_6$D$_6$, 400 MHz, ppm): δ 7.27−6.77 (m, 4H, Ph-*H*), 2.27 (s, 6H, −Ph-(C*H*$_3$)$_2$), 2.02 (dd, 4H, −C*H*-(CH$_3$)$_2$) 1.52 (s, 6H, −C(C*H*$_3$)$_2$), 1.12−0.99 (m, 24H, −CH−C*H*$_3$), 0.37(s, 18H, −Si-(C*H*$_3$)$_3$), −0.01(d, 4H, −C*H*$_2$-Si−). ^{13}C NMR (C$_6$D$_6$, 100 MHz, ppm): δ 4.8 (s, −Si(CH$_3$)$_3$), 19.6 (d, *J* = 12.2 Hz, CH(CH$_3$)$_2$)), 19.6 (d, *J* = 8.1 Hz, CH(CH$_3$)$_2$), 21.0 (s, CH(CH$_3$)$_2$), 23.8 (d, *J* = 10.1 Hz, ArCH$_3$), 28.8 (s, ArC(CH$_3$)$_2$), 36.6 (s, ArC(CH$_3$)$_2$), 49.4 (d, *J* = 10.1 Hz, −CH$_2$-Si−), 111.9 (d, *J* = 21.2 Hz, ArC), 126.8 (s, ArC), 128.6 (s, ArC), 130.6 (s, ArC), 132.9 (s, ArC), 154.7 (s, ArC). ^{31}P NMR (C$_6$D$_6$, 162 MHz, ppm): δ 1.19 (d, *J* = 85.9 Hz). Anal. Calcd for C$_{37}$H$_{66}$NP$_2$Si$_2$Y: C 60.71, H 9.09, N 1.91; Found: C 60.95, H 9.15, N 1.89.

*($^{acri\text{-}iPr}$PNP)Lu(CH$_2$SiMe$_3$)$_2$ (**1-Lu**).* A mixture of ($^{acri\text{-}iPr}$PNP)Li(THF) (298.6 mg, 0.6 mmol) and LuCl$_3$(THF)$_3$ (268.6 mg, 0.6 mmol) in toluene was stirred at room temperature for 1.5 h, and then the toluene solution of LiCH$_2$TMS (113.0 mg, 1.2 mmol) was added to the reaction mixture. Solvent was removed in a vacuum after 2 h, and the desired product ($^{i\text{-}Pr}$PNP)Lu(CH$_2$SiMe$_3$)$_2$ was obtained as a yellow powder after washing with cooled *n*-hexane and drying under a vacuum (311.1 mg, 63.4%). ^{1}H NMR (C$_6$D$_6$, 400 MHz, ppm): δ 7.29−6.76 (m, 4H, Ph-*H*), 2.25 (s, 6H, −Ph-(C*H*$_3$)$_2$), 2.10 (q, 4H, −C*H*-(CH$_3$)$_2$) 1.53 (s, 6H, −Ph-(C*H*$_3$)$_2$), 1.12−0.98 (m, 24H, −Ph-(C*H*$_3$)$_2$), 0.35(s, 18H, −Si-(C*H*$_3$)$_3$), −0.24(s, 4H, −C*H*$_2$-Si-). ^{13}C NMR (C$_6$D$_6$, 100 MHz, ppm): δ 5.0 (s, −Si(CH$_3$)$_3$), 19.4 (d, *J* = 19.2 Hz, CH(CH$_3$)$_2$)), 19.5 (d, *J* = 7.1 Hz, CH(CH$_3$)$_2$), 21.0 (s, CH(CH$_3$)$_2$), 24.1 (d, *J* = 12.1 Hz, ArCH$_3$), 29.6 (s, ArC(CH$_3$)$_2$), 36.6 (s, ArC(CH$_3$)$_2$), 57.3 (s, −CH$_2$-Si-), 111.5 (d, *J* = 23.2 Hz, ArC), 126.9 (s, ArC), 128.9 (s, ArC), 130.8 (s, ArC), 132.9 (s, ArC), 154.7 (s, ArC). ^{31}P NMR (C$_6$D$_6$, 162 MHz, ppm): δ 12.26 (s). Anal. Calcd for C$_{37}$H$_{66}$LuNP$_2$Si$_2$: C 54.33, H 8.13, N 1.71. Found: C 54.65, H 8.15, N 1.79.

*($^{acri\text{-}Ph}$PNP)Y(CH$_2$SiMe$_3$)$_2$(THF) (**2-Y**).* To a solution of $^{acri\text{-}Ph}$PNP (484.6 mg, 0.8 mmol) in dry toluene, the toluene solution of Y(CH$_2$SiMe$_3$)$_3$(THF)$_2$ (415.6 mg, 0.8 mmol) was added slowly at room temperature. Solvent was removed in a vacuum after stirring for 2 h, and the desired product ($^{acri\text{-}Ph}$PNP)Y(CH$_2$SiMe$_3$)$_2$(THF) (**2-Y**) was isolated as a yellow solid after washing with cooled *n*-hexane and drying under a vacuum (385.1 mg, 50.7%). ^{1}H NMR (C$_6$D$_6$, 400 MHz, ppm): δ 7.27−6.81 (m, 24H, Ph-*H*), 3.79 (t, 4H, *THF*), 2.01 (s, 6H, −Ph-(C*H*$_3$)$_2$), 1.58 (br, 4H, *THF*), 0.83 (t, 6H, −C(C*H*$_3$)$_2$), 0.25 (s, 18H, −Si-(C*H*$_3$)$_3$), −0.16 (s, 4H, −Si-C*H*$_2$−). ^{13}C NMR (C$_6$D$_6$, 100 MHz, ppm): δ 4.9 (s, −Si(CH$_3$)$_3$), 21.0 (s, ArCH$_3$), 21.5 (s, ArC(CH$_3$)$_2$), 25.1 (s, β-CH$_2$, THF), 37.0 (s, ArC(CH$_3$)$_2$), 41.1 (d, *J* = 36.4 Hz, −CH$_2$-Si-), 70.9 (s, α-CH$_2$, THF), 117.7 (d, *J* = 22.2 Hz, ArC), 125.7 (s, ArC), 128.6 (s, ArC), 128.7 (d, *J* = 8.1 Hz, ArC), 129.3 (s, ArC), 132.6 (s, ArC), 133.2 (d, *J* = 36.4 Hz, ArC), 134.7 (br, ArC), 137.9 (s, ArC), 153.1 (d, *J* = 23.2 Hz, ArC). ^{31}P NMR (C$_6$D$_6$, 162 MHz, ppm): δ −12.48 (d, *J* = 47.0 Hz). Anal. Calcd for C$_{53}$H$_{66}$NOP$_2$Si$_2$Y: C 67.71, H 7.08, N 1.49. Found: C 67.95, H 7.11, N 1.50.

*($^{acri\text{-}Ph}$PNP)Lu(CH$_2$SiMe$_3$)$_2$(THF) (**2-Lu**).* The mixture solution of $^{acri\text{-}Ph}$PNP (484.6 mg, 0.8 mmol) and Lu(CH$_2$SiMe$_3$)$_3$(THF)$_2$ (487.9 mg, 0.8 mmol) in dry toluene was slowly warmed up to 50 °C under a N$_2$ atmosphere. Solvent was removed in a vacuum after stirring for 2 h, and the desired product was isolated as a yellow solid after washing with *n*-hexane and drying under a vacuum (412.0 mg, 0.40 mmol, 50.2%). ^{1}H NMR (C$_6$D$_6$, 400 MHz, ppm): δ 7.49−6.57 (m, 24H, Ph-*H*), 3.75 (t, 4H, *THF*), 2.01 (s, 4H, *THF*), 1.96 (s, 6H, −Ph-(C*H*$_3$)$_2$), 1.11 (br, 6H, −C (C*H*$_3$)$_2$), 0.22 (s, 18H, −Si-(C*H*$_3$)$_3$), 0.00 (s, 4H, −Si-C*H*$_2$−). ^{13}C NMR (C$_6$D$_6$, 100 MHz, ppm): δ 4.7 (s, −Si(CH$_3$)$_3$), 20.7 (s, ArCH$_3$), 21.1 (s, ArC(CH$_3$)$_2$), 24.8 (s, β-CH$_2$, THF), 36.7 (s, ArC(CH$_3$)$_2$), 45.1 (s, −CH$_2$-Si-), 70.8 (s, α-CH$_2$, THF), 117.5 (d, *J* = 23.2 Hz, ArC), 125.4 (s, ArC), 128.4 (d, *J* = 4.4 Hz, ArC), 129.1 (s, ArC), 132.3 (s, ArC), 133.2 (d, *J* = 6.1 Hz, ArC), 133.5 (br, ArC), 134.2 (d, *J* = 16.2 Hz, ArC), 153.4 (d, *J* = 22.2 Hz, ArC). ^{31}P NMR (C$_6$D$_6$, 162 MHz, ppm): δ −7.47 (s). Anal. Calcd for C$_{53}$H$_{66}$LuNOP$_2$Si$_2$: C 62.03, H 6.48, N 1.36. Found: C 62.29, H 6.41, N 1.38.

Polymerization of Isoprene and β-Myrcene with 1-Y/[Ph$_3$C][B(C$_6$F$_5$)$_4$]. Under a nitrogen atmosphere, complex **1-Y** (20.0 μmol in 4.0 mL toluene) and [Ph$_3$C][B(C$_6$F$_5$)$_4$] (20.0 μmol in 2.0 mL toluene) were placed into a bottle and stirred for 5 min. Then isoprene (0.68 g, 10 mmol) or β-myrcene (1.36 g, 10 mmol) was added and vigorously stirred for 10 min. The viscous solution was poured into a large quantity (60.0 mL) of methanol to give polyisoprene or polymyrcene solids that were dried under a vacuum at 60 °C to a constant weight (100% yield).

Calculation of the selectivity of polyisoprene:

According to the ^1H NMR spectrum of the polyisoprene: $3,4\ (\%) = (1/2I_{4.78})/(I_{5.14} + 1/2I_{4.78})$; $1,4\ (\%) = I_{5.14}/(I_{5.14} + 1/2I_{4.78})$

According to the ^{13}C NMR spectrum of the polyisoprene: *cis*-1,4/*trans*-1,4 (%) = $I_{23.4}/I_{15.9}$.

Calculation of the selectivity of polymyrcene:

According to the ^1H NMR spectrum of the polymyrcene: $3,4\ (\%) = I_{4.81}/(I_{5.13} + 1/2I_{4.81})$; $1,4(\%) = (I_{5.13} - 1/2I_{4.81})/(I_{5.13} + 1/2I_{4.81})$

According to the ^{13}C NMR spectrum of the polymyrcene: *cis*-1,4/*trans*-1,4 (%) = $I_{37.1}/I_{37.5}$.

Copolymerization of Isoprene and Butadiene with 1-Y/[Ph_3C][$B(C_6F_5)_4$]. Under a nitrogen atmosphere, **1-Y** (5.0 μmol in 3.0 mL toluene) and [Ph_3C][$B(C_6F_5)_4$] (5.0 μmol in 2.0 mL toluene) were placed in a bottle and stirred for 5 min. The mixture of isoprene and butadiene (5 mL) was added into the flask, and the polymerization was carried out for 10 min. The viscous reaction mixture was poured into a large quantity (100 mL) of methanol to give white solids of a copolymer that were dried under a vacuum at 60 °C to a constant weight.

ASSOCIATED CONTENT

Supporting Information

The Supporting Information is available free of charge at https://pubs.acs.org/doi/10.1021/acs.inorgchem.0c03274.

^1H/^{13}C NMR spectra of complexes (PDF)

Accession Codes

CCDC 2042088−2042089 contain the supplementary crystallographic data for this paper. These data can be obtained free of charge via www.ccdc.cam.ac.uk/data_request/cif, or by emailing data_request@ccdc.cam.ac.uk, or by contacting The Cambridge Crystallographic Data Centre, 12 Union Road, Cambridge CB2 1EZ, UK; fax: +44 1223 336033.

AUTHOR INFORMATION

Corresponding Author

Xiaochao Shi − *Department of Polymer Materials, College of Materials Science and Engineering, Shanghai University, Shanghai 200444, China*; orcid.org/0000-0001-5178-7972; Email: xcshi@shu.edu.cn

Authors

Fen You − *Department of Polymer Materials, College of Materials Science and Engineering, Shanghai University, Shanghai 200444, China*

Jingjing Zhai − *Department of Polymer Materials, College of Materials Science and Engineering, Shanghai University, Shanghai 200444, China*

Yat-Ming So − *Department of Chemistry, The Hong Kong University of Science and Technology, Hong Kong, China*

Complete contact information is available at: https://pubs.acs.org/10.1021/acs.inorgchem.0c03274

Notes

The authors declare no competing financial interest.

ACKNOWLEDGMENTS

This work was supported by the National Natural Science Foundation of China (21704060) and the Program for Professor of Special Appointment (Eastern Scholar) at Shanghai Institutions of Higher Learning.

REFERENCES

(1) For selected review, see: (a) Fischbach, A.; Anwander, R. Rare-earth metals and aluminum getting close in Ziegler-type organometallics. *Adv. Polym. Sci.* **2006**, *204*, 155−281. (b) Nishiura, M.; Hou, Z. M. Novel polymerization catalysts and hydride clusters from rare-earth metal dialkyls. *Nat. Chem.* **2010**, *2*, 257−268. (c) Nishiura, M.; Guo, F.; Hou, Z. M. Half-sandwich rare-earth-catalyzed olefin polymerization, carbometalation, and hydroarylation. *Acc. Chem. Res.* **2015**, *48*, 2209−2220. (d) Huang, J. M.; Liu, Z. H.; Cui, D. M.; Liu, X. L. Precisely controlled polymerization of styrene and conjugated dienes by Group 3 single-site catalysts. *ChemCatChem* **2018**, *10*, 42−61. (e) Hollfelder, C. O.; Jende, L. N.; Diether, D.; Zelger, T.; Stauder, R.; Maichle-Mössmer, C.; Anwander, R. 1,3-Diene polymerization mediated by homoleptic tetramethylaluminates of the rare-earth metals. *Catalysts* **2018**, *8*, 61−81.

(2) (a) Miyazawa, A.; Kase, T.; Soga, K. *Cis*-specific living polymerization of 1,3-butadiene catalyzed by alkyl and alkylsilyl substituted cyclopentadienyltitanium trichlorides with MAO. *Macromolecules* **2000**, *33*, 2796−2800. (b) Boisson, C.; Monteil, V.; Ribour, D.; Spitz, R.; Barbotin, F. Lanthanidocene catalysts for the homo- and copolymerization of ethylene with butadiene. *Macromol. Chem. Phys.* **2003**, *204*, 1747−1754. (c) Miyazawa, A.; Kase, T.; Hashimoto, K.; Choi, J. C.; Sakakura, T.; Ji-zhu, J. Polymerization of 1,3-butadiene catalyzed by half-sandwich titanocenes bearing a coordinative ether and ester side chain on the Cp Ring and MAO. *Macromolecules* **2004**, *37*, 8840−8845. (d) Kaita, S.; Yamanaka, M.; Horiuchi, A. C.; Wakatsuki, Y. Butadiene polymerization catalyzed by lanthanide metallocene-alkylaluminum complexes with cocatalysts: metal-dependent control of 1,4-*cis*/*trans* stereoselectivity and molecular weight. *Macromolecules* **2006**, *39*, 1359−1363.

(3) (a) Monteil, V.; Spitz, R.; Boisson, C. Polymerization of butadiene and copolymerization of butadiene with styrene using neodymiurn amide catalysts. *Polym. Int.* **2004**, *53*, 576−581. (b) Sugiyama, H.; Gambarotta, S.; Yap, G. P. A.; Wilson, D. R.; Thiele, S. K. H. Preparation of an active neodymium catalyst for regioselective butadiene *cis*-polymerization supported by a dianionic modification of the 2,6-diiminopyridine ligand. *Organometallics* **2004**, *23*, 5054−5061. (c) Arndt, S.; Beckerle, K.; Zeimentz, P. M.; Spaniol, T. P.; Okuda, J. Cationic yttrium methyl complexes as functional models for polymerization catalysts of 1,3-dienes. *Angew. Chem., Int. Ed.* **2005**, *44*, 7473−7477. (d) Zhang, L. X.; Suzuki, T.; Luo, Y.; Nishiura, M.; Hou, Z. M. Cationic alkyl rare-earth metal complexes bearing an ancillary bis(phosphinophenyl)amido ligand: a catalytic system for living *cis*-1,4-polymerization and copolymerization of isoprene and butadiene. *Angew. Chem., Int. Ed.* **2007**, *46*, 1909−1913. (e) Visseaux, M.; Mainil, M.; Terrier, M.; Mortreux, A.; Roussel, P.; Mathivet, T.; Destarac, M. Cationic borohydrido-neodymium complex: synthesis, characterization and its application as an efficient pre-catalyst for isoprene polymerization. *Dalton Trans.* **2008**, *34*, 4558−4561. (f) Li, D. F.; Li, S. H.; Cui, D. M.; Zhang, X. Q. beta-Diketiminato rare-earth metal complexes. Structures, catalysis, and active species for highly *cis*-1,4-selective polymerization of isoprene. *Organometallics* **2010**, *29*, 2186−2193. (g) Lv, K.; Cui, D. M. CCC-pincer bis(carbene) lanthanide dibromides. catalysis on highly *cis*-1,4-selective polymerization of isoprene and active species. *Organometallics* **2010**, *29*, 2987−2993. (h) Yang, Y.; Lv, K.; Wang, L. F.; Wang, Y.; Cui, D. M. Isoprene polymerization with aminopyridinato ligand supported rare-earth metal complexes. Switching of the regio- and stereoselectivity. *Chem. Commun.* **2010**, *46*, 6150−6152. (i) Li, L.; Wu, C. J.; Liu, D. T.; Li, S. H.; Cui, D. M. Binuclear rare-earth-metal alkyl complexes ligated by phenylene-bridged beta-diketiminate ligands: synthesis, characterization, and catalysis toward isoprene polymerization. *Organometallics* **2013**, *32*, 3203−3209. (j) Zhang, G. C.; Wei, Y.; Guo, L. P.; Zhu, X. C.; Wang, S. W.; Zhou, S. L.; Mu, X. L. Dinuclear rare-earth metal alkyl complexes supported by indolyl ligands in mu-eta(2):eta(1):eta(1) hapticities and their high catalytic activity for isoprene 1,4-*cis*-polymerization. *Chem. - Eur. J.* **2015**, *21*, 2519−2526. (k) Li, L.; Li, S. H.; Cui, D. M. Highly *cis*-1,4-selective living polymerization of 3-methylenehepta-1,6-diene and its subse-

quent thiol-ene reaction: an efficient approach to functionalized diene-based elastomer. *Macromolecules* **2016**, *49*, 1242−1251. (l) Zhang, G. C.; Deng, B. J.; Wang, S. W.; Wei, Y.; Zhou, S. L.; Zhu, X. L.; Huang, Z. M.; Mu, X. L. Di and trinuclear rare-earth metal complexes supported by 3-amido appended indolyl ligands: synthesis, characterization and catalytic activity towards isoprene 1,4-*cis* polymerizationt. *Dalton Trans.* **2016**, *45*, 15445−15456. (m) Yang, F. Z.; Li, X. F. Novel cationic rare earth metal alkyl catalysts for precise olefin polymerization. *J. Polym. Sci., Part A: Polym. Chem.* **2017**, *55*, 2271−2280. (n) Yu, C.; Zhou, D. H.; Yan, X. Q.; Gao, F.; Zhang, L.; Zhang, S. W.; Li, X. F. *Cis*-1,4-polymerization of isoprene by 1,3-bis(oxazolinymethylidene)isoindoline-ligated rare-earth metal dialkyl complexes. *Polymers* **2017**, *9*, 531−541. (o) Pan, Y.; Li, W. Q.; Wei, N. N.; So, Y. M.; Li, Y.; Jiang, K.; He, G. H. Anilido-oxazoline-ligated rare-earth metal complexes: synthesis, characterization and highly *cis*-1,4-selective polymerization of isoprene. *Dalton Trans.* **2019**, *48*, 3583−3592.

(4) Gao, W.; Cui, D. M. Highly *cis*-1,4 selective polymerization of dienes with homogeneous Ziegler-Natta catalysts based on NCN-pincer rare earth metal dichioride precursors. *J. Am. Chem. Soc.* **2008**, *130*, 4984−4991.

(5) Li, X. F.; Nishiura, M.; Hu, L. H.; Mori, K.; Hou, Z. M. Alternating and random copolymerization of isoprene and ethylene catalyzed by cationic half-sandwich scandium alkyls. *J. Am. Chem. Soc.* **2009**, *131*, 13870−13882.

(6) (a) Zhang, L. X.; Suzuki, T.; Luo, Y.; Nishiura, M.; Hou, Z. M. Cationic alkyl rare-earth metal complexes bearing an ancillary bis(phosphinophenyl)amido ligand: a catalytic system for living *cis*-1,4-polymerization and copolymerization of isoprene and butadiene. *Angew. Chem., Int. Ed.* **2007**, *46*, 1909−1913. (b) Wang, L. F.; Cui, D. M.; Hou, Z. M.; Li, W.; Li, Y. Highly *cis*-1,4-selective living polymerization of 1,3-conjugated dienes and copolymerization with ε-caprolactone by bis(phosphino)carbazolide rare-earth-metal complexes. *Organometallics* **2011**, *30*, 760−767.

(7) (a) Liang, L. C. Metal complexes of chelating diarylamido phosphine ligands. *Coord. Chem. Rev.* **2006**, *250*, 1152−1177. (b) Mindiola, D. J. Oxidatively induced abstraction reactions. a synthetic approach to low-coordinate and reactive early transition metal complexes containing metal-ligand multiple bonds. *Acc. Chem. Res.* **2006**, *39*, 813−821.

(8) (a) Yoo, C. H.; Lee, Y. H. A T-shaped nickel(I) metalloradical species. *Angew. Chem., Int. Ed.* **2017**, *56*, 9502−9506. (b) Sahoo, D.; Yoo, C. H.; Lee, Y. H. Direct CO_2 addition to a Ni(0)−CO species allows the selective generation of a nickel(II) carboxylate with expulsion of CO. *J. Am. Chem. Soc.* **2018**, *140*, 2179−2185.

(9) Pingen, D.; Choi, J. H.; Allen, H.; Murray, G.; Ganji, P.; Van Leeuwen, P. W. N. M.; Prechtl, M. H. G.; Vogt, D. Amide versus amine ligand paradigm in the direct amination of alcohols with Ru-PNP complexes. *Catal. Sci. Technol.* **2018**, *8*, 3969−3976.

(10) Mo, Z. B.; Shima, T.; Hou, Z. M. Synthesis and diverse *trans*formations of a dinitrogen dititanium hydride complex bearing rigid acridane-based PNP-pincer ligands. *Angew. Chem., Int. Ed.* **2020**, *59*, 8635−8644.

(11) Liu, H.; Wang, N. D.; Du, D. M. Direct experimental evidence for the priority of flexible ligand skeleton in asymmetric Friedel-Crafts alkylation of indole with nitroalkenes. *Lett. Org. Chem.* **2010**, *7*, 114−120.

(12) (a) Georges, S.; Touré, A. O.; Visseaux, M.; Zinck, P. Coordinative chain transfer copolymerization and terpolymerization of conjugated dienes. *Macromolecules* **2014**, *47*, 4538−4547. (b) Liu, B.; Li, L.; Sun, G.; Liu, D.; Li, S.; Cui, D. Isoselective 3,4-(co)polymerization of bio-renewable myrcene using NSN-ligated rare-earth metal precursor: an approach to a new elastomer. *Chem. Commun.* **2015**, *51*, 1039−1041. (c) Ren, X.; Guo, F.; Fu, H.; Song, Y.; Li, Y.; Hou, Z. Scandium-catalyzed copolymerization of myrcene with ethylene and propylene: convenient syntheses of versatile functionalized polyolefins. *Polym. Chem.* **2018**, *9*, 1223−1233. (d) Li, W. Q.; Jiang, X. X.; So, Y. M.; He, G. H.; Pan, Y. Lutetium and yttrium complexes supported by an anilido-oxazoline ligand for polymerization of 1,3-conjugated dienes and epsilon-caprolactone. *New J. Chem.* **2020**, *44*, 121−128.